Mat. Res. Soc. Symp. Proc. Vol. 704 © 2002 Materials Research Society

Light scattering by isolated nanoparticles with arbitrary shapes

Cecilia Noguez, Iván O. Sosa, and Rubén G. Barrera
Instituto de Física, Universidad Nacional Autónoma de México, Apartado Postal 20-364, México D.F., México.

ABSTRACT

Using the Discrete Dipole Approximation we have studied the optical properties of different isolated nanoparticles with arbitrary shapes. We have investigated the main features in the optical spectra, depending of the geometry and size of such nanoparticles. We present and discuss our results in terms of the scattering, extinction and absorption optical coefficients, which can be directly compared with experiments. The results are discussed in terms of the optical signature of each nanoparticle depending of its size and shape.

INTRODUCTION

In the last few years, a lot of effort has been made in the development of the science and technology at the nanometer scale, covering from growth and characterization to device processing. The fabrication of nanostructures requires a deeper understanding of physical phenomena involved at this scale. In particular, the shape and size of such low-dimensional structures are crucial parameters to determine their physical properties. For example, low-dimensional quantum structures have shown to have unique optical properties, which have been employed in the fabrication of new opto-electronic devices [1].

The estimation of the shape and size of nanoparticles can be done using several structural characterization techniques, such as Atomic Force Microscopy (AFM), Scanning Tunneling Microscopy (STM), Transmission Electron Microscopy (TEM), Reflection High-Energy Electron Diffraction (RHEED) [2-5], and optical spectroscopies such as absorption spectroscopy, Surface Enhanced Raman Scattering (SERS), and Differential Reflectance (DR) [6-8]. Different shapes of nanoparticles have been observed using these techniques, such as spheres, spheroids, lens-shaped, cone-shaped, pyramids with different facets, and truncated pyramids [9-12]. The predicted values of the quantum dot ground state and excited states will be obtained accurately only if the correct shape and size of the particle is known. In particular, a variety of size and shape dependent results are found in optical studies that relate the surface plasmon excitons, and significant enhancement in Raman intensities of the peaks in the absorption and Raman excitation profiles [13]. However, an exact experimental determination of size and shape parameters of a given particle at present is still controversial.

Structural characterization techniques like AFM , RHEED, or TEM are useful tools to qualitatively characterize the shape and size parameters of nanoparticle. However, these tools have some limitations to resolve such parameters of nanoparticles. One of the main limitations is that in most cases the growth and characterization of nanoparticles are made in different ambient. This is a serious problem since the properties of the nanoparticles are ambient dependent. On the other hand, structural techniques can substantially modify the properties of the nanoparticle, and under some conditions these tools could destroy the samples. Furthermore, the growth and

characterization of the parameters of such nanoparticles are made at different times, which can be also an additional uncontrollable variable of the physical properties. All these limitations make desirable the development of a characterization tool that can accomplish its functions in the same ambient conditions, at a real time, and in a non-destructive way. These attributes can be achieve employing optical characterization tools, since optical spectroscopies have been very useful within this context, due to their non-destructive and real-time character and in situ potentiality [6-8], which are not usually present in structural characterization techniques, such as AFM , RHEED, or TEM. These properties of optical characterization tools will allow to control the growth of nanoparticles at the same time, and it will possible to correct the shape and size of such nanoparticle. In the future, this fact will be crucial in the development of the nanosciences and its technological applications.

In this paper we present a theoretical study of the optical properties of silver and gold isolated nanoparticles with different shapes and sizes. Gold and silver nanometric size particles are of interest since their physical and chemical properties are very different from bulk metals. One of our goals is to relate the main peaks of the optical spectra of these nanoparticles to shape and size parameters, as well as their material properties. We believe that this study can be help to determine and optimize nanoparticle physical properties during and after growth.

FORMALISM

In this work, the nanoparticles of interest are typically large enough that we can accurately apply the classical electromagnetic theory to describe their interaction with light. But they are small enough so we can observe strong variations in the optical properties with particle size, shape, and local environment. Because of the complexity of the systems being studied, efficient computational methods capable of treating large materials are essential. In the last few years, have been developed several numerical methods to find the optical properties of small particles such as the Discrete Dipole Approximation (DDA), T-matrix methods, Spectral Representation methods (SR) and more. In this work we employed DDA, which is a well suitable technique for studying scattering and absorption of electromagnetic radiation by particles with sizes of the order of the wavelength or less. DDA has been applied to a broad range of problems, including interstellar dust grains, ice crystals in the atmosphere in the Earth, interplanetary dust, human blood cells, surface features of semiconductors, metal nanoparticles and their aggregates, and more. DDA was first introduced by Purcell and Pennypacker [14], and has been subjected to several improvements, in particular those made by Draine, and collaborators [15].

Discrete Dipole Approximation (DDA)

The main idea behind DDA is to approximate a target, in our case the nanoparticle, by an array of polarizable points or dipoles. Once the localization and polarizability of each dipole are specified, the calculation of the scattering and absorption coefficients by the dipole array can be done, depending only on the accuracy of the computational hardware.

Suppose we have an array of N polarizable points $\{\mathbf{R}_i\}$, $i = 1, 2, \ldots, N$, each one characterized by a polarizability complex tensor α_i. The system is excited by a monochromatic incident wave $\mathbf{E}_{\text{inc}} e^{i\omega t}$, where ω is the angular frequency and t denotes time. Each dipole of the system is

subject to an electric field that can be divided into two contributions: (i) the incident radiation field, plus (ii) the radiation field resulting from all of the other induced dipoles. The sum of both fields is the so called local field at each dipole given by

$$\mathbf{E}_{i,\,\text{local}} = \mathbf{E}_{i,\,\text{inc}} + \mathbf{E}_{i,\,\text{dip}} = \mathbf{E}_0 e^{i\mathbf{k}\cdot\mathbf{r}} - \sum_{i\neq j} \mathbf{A}_{ij}\cdot\mathbf{P}_j \quad , \tag{1}$$

where $\mathbf{P}_i$ is the dipole moment of the ith element, and $\mathbf{A}_{ij}$ is the dipole-dipole interaction matrix, given by

$$\mathbf{A}_{ij}\cdot\mathbf{P}_j = \frac{e^{ikr_{ij}}}{r_{ij}^3}\left[k^2\mathbf{r}_{ij}\times(\mathbf{r}_{ij}\times\mathbf{P}_j) + \frac{(1-ikr_{ij})}{r_{ij}^2}[r_{ij}^2\mathbf{P}_j - 3\mathbf{r}_{ij}(\mathbf{r}_{ij}\cdot\mathbf{P}_j)]\right]. \tag{2}$$

Here $k = \omega/c = 2\pi/\lambda$, $\mathbf{r}_{ij} = \mathbf{r}_j - \mathbf{r}_i$, and $r_{ij} = |\mathbf{r}_{ij}|$, and c is the speed of light, and λ is the wavelength of the incident light. Once we have solved the $3N$-coupling complex linear equations given by $\mathbf{P}_i = \alpha_i\cdot\mathbf{E}_{i,\,\text{loc}}$, have each dipole moment, and then we can find the extinction and absorption cross sections for a target given by the following expressions

$$C_{\text{ext}} = \frac{4\pi k}{|\mathbf{E}_0|^2}\sum_{i=1}^{N}\text{Im}(\mathbf{E}_{i,\,\text{inc}}^{*}\cdot\mathbf{P}_i), \qquad C_{\text{abs}} = \frac{4\pi k}{|\mathbf{E}_0|^2}\sum_{i=1}^{N}\left[\text{Im}(\mathbf{P}_i\cdot(\alpha_i^{-1})^{*}\mathbf{P}_i^{*}) - \frac{1}{3}k^3|\mathbf{P}_i|^2\right], \tag{3}$$

where (*) means complex conjugated. The scattering cross section can be obtained using the following relation, $C_{\text{sca}} = C_{\text{ext}} - C_{\text{abs}}$.

There is some arbitrariness in the construction of the array of dipole points that represent a solid target of a given geometry. For example, it is not obvious how many dipoles are required to adequately approximate the target, or which is the best choice of dipole polarizabilities. We can choose the separation between dipoles d such that $d<<\lambda$, such that we can asign the polarizability for each particle i in vacuum, using the Clausius-Mossotti. Now the question is, how many dipoles we need to mimic the continuum particle with an array of discrete dipoles? The answer is not straightforward, since we have to consider the convergence of the physical quantities as a function of the dipole number. We found that for an arbitrary geometry $N \geq 10^4$ is a good number. However, we have a matrix of $(3N)^2$ complex elements which would require a large amount of computational effort.

In this work we have employed the program adapted by Draine and Flatau to solve the complex linear equations found from DDA. To directly solve the complex linear equations we would require a tremendous computer capabilities, however, we can use iterative techniques to approximately compute **P**. This algorithm, called DDSCAT, uses a periodic lattice where the dipoles are located, then it is possible to use fast Fourier transform techniques to evaluate matrix-vector products, which allows the hole computation of the final **P** for a large number of dipoles. Finally, if we want a variation of the phase of the incoming field radiation of less than a radian between first-neighbors dipoles, we will need to satisfy the relation $|\sqrt{\varepsilon}|kd \ll 1$. Then, it is also clear that we would require a large N or large wavelengths, or a small refractive index $\sqrt{\varepsilon}$. For a complete description of DDA and DDSCAT code, the reader can consult References [15,16].

RESULTS AND DISCUSSION

We have calculated the extinction and absorption coefficients per surface unit area A, defined by $Q_{ext/abs} = C_{ext/abs}/A$, as a function of λ for silver and gold nanoparticles with different geometries like spheres, ellipsoids and cubes, and different sizes. We have represented or mimic the nanoparticles with thousands of dipoles $N>10^4$, in order to have a good convergence of the physical properties studied here.

In Fig. 1(a) we show Q_{ext} as a function of λ is shown for silver spheres of for silver spheres of 50 nm (solid line), 100 nm (dotted line), 150 nm (dashed line), and 200 nm (dashed-dotted line). The spheres are made of silver and mimic with 65,000 dipoles. In Fig. 1(a), we can observe that at about 320 nm all the Q_{ext} spectra have a local minimum that corresponds to the wavelenhg at which intra-band electron transitions on silver start. These intra-band transitions give rise to the peak in the Q_{abs} spectra at about 350 nm, this is shown in Fig. 1(b). In the Q_{ext} spectra a maximum at 400 nm is observed which is more pronounced for the nanoparticle with the smallest radio. This maximum diminishes as the size of the particle increases. However for larger wavelengths, the spectrum for the nanoparticle of 50 nm decays very quickly, while the spectra of the other nanoparticles do not show the same behavior.

In Fig. 1(b) we show the Q_{abs} spectra as a function of λ for the silver spheres described in Fig. 1(a). In this case we can observe in the Q_{abs} spectra, very large and sharp peaks above 450 nm for spheres of 100, 150 and 200 nm. These large peaks are due to the lack of convergence of the calculations, such that they have no any physical explanation. As is shown in Fig. 1(c), where Q_{ext} for the sphere of 100 nm is plot as a function of λ these large peaks are washed out as the number of dipoles in the calculation is increased dramatically from 65,000 to 221,000. This lack of convergence is particularly observed in metal particles due to the fact that for large wavelengths the dielectric function of silver, and in general for metals, is negative and very large. Taken into account these considerations, we can explain the Q_{ext} spectra for $\lambda > 350$ nm as light-scattering effects for the spheres larger than 50 nm. Furthermore, in Fig. 1(a), we can see that light scattering is less intense for small nanospheres, as it is expected.

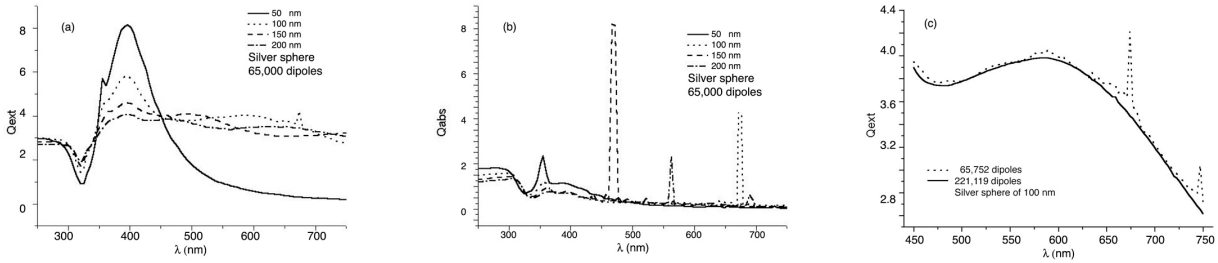

Figure 1. Q_{ext} and Q_{abs} as a function of λ for nanospeheres of different sizes.

In Fig. 2 we show Q_{ext} for (a) gold and (b) silver ellipsoidal nanoparticles where the incident electromagnetic field is taken perpendicular (solid line) and parallel (dashed line) to the major axis of the ellipsoid. The ellipsoidal nanoparticles have a major semiaxis of 3 nm, with a ratio 2:1 between minor and major axis, and are mimic with 12,600 dipoles that resembles well the physical properties of such nanoparticles. As it is expected, the main contribution to Q_{ext} comes

from the excited surface plasmon, which its location and intensity depend on the particular geometry of each nanoparticle. For both materials, the main contribution to Q_{ext} corresponds to an external field parallel to the major axis of the ellipsoid. For such small nanoparticles the peaks in the Q_{ext} spectra are dominated by light absorption processes due to the geometrical properties of the particle. On the other hand, the intensity and sharpness of the spectra is dominated by the material properties of the particle. Both ellipsoidal nanoparticles show a main peak for both external fields. In particular, for a external field parallel to the major semiaxis the spectra show a large peak at wavelengths above 450 nm, and also show a small peak or shoulder at wavelengths below 300 nm. For the silver particle, the main peak is more intense and sharper than the peak corresponding to the gold particle. The second peak or shoulder of the silver particle is ten times less intense than the main peak, while for the gold nanoparticle the second peak is wider and more intense in comparison to the main peak. For both nanoparticles, the structure at lower wavelengths (λ< 300 nm) is due to intra-band electron transitions on these metals.

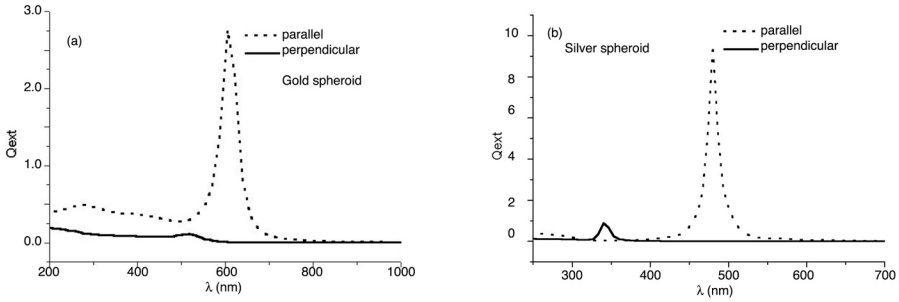

Figure 2. Q_{ext} as a function of λ for ellipsoidal nanoparticles of (a) gold and (b) silver.

In Fig. 3(a) and (b) we show Q_{ext} and Q_{abs} respectively, as a function of λ for cubic nanoparticles made of silver of 50 nm (solid line) and of 150 nm (dashed line) of side. Both cubic nanoparticles are mimic with 65,000 dipoles. The large peak in fig.3(b) at about λ~720 nm is due to the lack of convergence in the calculation. This peak can be washed out using a larger amount of dipoles, however it does not affect the discussion of the present results, since the main effects are observed at shorter wavelengths. We can observe that the cubic shape of the nanoparticles show a rich structure in Q_{ext} and Q_{abs} , which were not observed for the previous spherical and spheroidal geometries. These peaks are due to the several kind of surface plasmons excited in the cubic nanoparticle . In Fig. 3(a), corresponding to Q_{ext} of the silver nanocube, we can observe that the peaks from λ=200 nm to λ<450 nm are due to the particular geometry of the nanoparticle since they are present for both of cubic nanoparticle, and these structure are predominant in the Q_{abs} spectra in Fig. 3(b). In a cube, we have that several surface plasmons can be excited in the faces of the cube. At larger λ<450 nm, the spectrum has contributions from the light scattering as well. As the size of the particle increases, this peak moves to larger wavelengths. The latter is confirmed in Fig.~3(b), since Q_{abs} shows contributions to the spectra only for λ<450 nm for both naoparticles. In Fig. 3(c) we show Q_{ext} for a gold cubic nanoparticle of side of 6 nm mimic with 110,500 dipoles, which size is very small compared with the wavelength of the incident light. Therefore, the whole structure of the spectrum is due to absorption effects only. In this case, the structure of several peaks found for silver nanoparticles is repleaced by a wide structure from λ=200 nm to about λ=600nm. This wide structure is due to surface plasmons which are affected by the intra-band transitions in gold which washed out the

fine structure of the surface plasmon excitations, since both effects are in the same range of wavelengths.

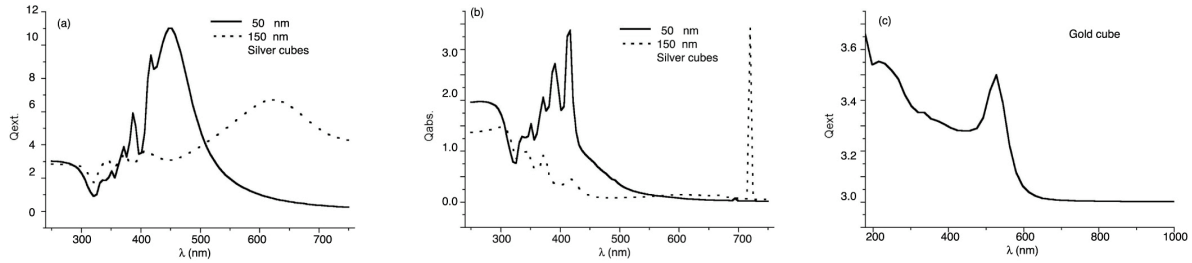

Figure 3. Q_{ext} and Q_{abs} as a function of for cubic nanoparticles.

CONCLUSIONS

Using the discrete dipole approximation we have calculated the main optical features of the extinction and absorption coefficients for nanoparticles made of silver and gold, of different sizes and shapes. We have studied the sphere, ellipsoid and cube nanoparticles of different size. We found that special features in the spectra can be attributed to either geometry or size, making optical spectroscopies very helpful in the characterization of nanoparticles during their grown.

ACKNOLWEDGEMENTS

This work has been partly supported by CONACyT and DGAPA-UNAM Mexico.

REFERENCES

1. See for example, Mater. Res. Bull. **23** (2), 31 (1998); and references therein.
2. B. Damilano, et al *J. of Crystal Growth*, **227-226,** 466 (2001)
3. M.J. Zheng, et al. *Semicond. Sci. Technol* **16**, 507 (2001)
4. TW Kim, et al. *Solid State Comm*. **118**, 465 (2001)
5. G.E. Cirlin, et al. *Material Scence and Engineering,* **B80,** 108 (2001)
6. C. E. Roman-Velazquez, et al., *MRS Symposium Proceedings* **581**, 485 (2000.
7. C. Beitia, Y. Borensztein, R. G. Barrera, C. E. Roman, C. Noguez, *Physica B* **279**, 25 (2000).
8. C. E. Roman, C. Noguez, R.G. Barrera, *Physical Review B*, **61**, 10427 (2000).
9. N. Liu, et al., Phys. Rev. Lett. **84**, 334 (2000).
10. J. Zou, X.Z. Liao, D.J.H. Cockayne, and R. Leon, Phys. Rev. B **59**, 12279 (1999).
11.W. Yang, H. Lee, T.J. Johnson, P.C. Sercel, and A.G. Norman, Phys. Rev. B **61**, 2784 (2000).
12. M. José Yacamán, et al., J. Vac. Sci. Technol. B **19**, 1091 (2001).
13. N. Félidj, J. Aubard, and G. L\'evi, J. Chem. Phys. **111**, 1195 (1999).
14. E.M. Purcell and C.R. Pennypacker, Astrophys. J. **186**, 705 (1973).
15. B.T. Draine, Astrophys. J. **333**, 848 (1998); B. T. Draine and J.J. Goodman, Astrophys. J. **405**, 685 (1993); B. T. Draine and P.J. Flatau, J. Opt. Am. A **11**, 1491 (1994).